



# The shallow metallicity gradient of the Triangulum galaxy and its time evolution

L. Magrini, D. Galli, and E. Corbelli

Istituto Nazionale di Astrofisica – Osservatorio Astronomico di Arcetri, Largo E. Fermi, 5,  
I-50125 Firenze, Italy  
e-mail: laura@arcetri.astro.it

**Abstract.** In the present work, we use the Triangulum Galaxy (hereafter M33) in the Local Group as prototype to study the chemical evolution of low surface brightness spiral galaxies, and trace their star formation and accretion histories. We examine oxygen and sulfur abundances of planetary nebulae, HII regions, and young stars, together with iron abundances in the old stellar population. Our chemical evolution model, that follows the time evolution of the gaseous and stellar disk of M33, well reproduces their observed radial distribution and predicts the time evolution of several elemental abundances, in agreement with observational constraints. Our best model is characterized by a continuous infall of gas on the disk, at a rate which today is  $\dot{M}_{\text{inf}} \approx 1 M_{\odot} \text{ yr}^{-1}$ , and did not vary much through cosmic time since the formation epoch of the galaxy disk. It can reproduce the relatively high star formation rate and the shallow chemical gradients observed. Supported by a large sample of high resolution observations for this galaxy, we conclude that the metallicity in the disk of M33 has increased with time at all radii, with a continuous flattening of the gradient over the last  $\sim 8$  Gyr.

**Key words.** Galaxies: abundances, evolution - Galaxies, individual: M33

## 1. Introduction

The Triangulum galaxy (M33) is a low-luminosity late-type spiral galaxy located in the LG at a distance of 840 kpc (Freedman et al. 1991). Its large angular size, together with its modest inclination ( $i = 54^{\circ}$ ), makes it particularly suitable for detailed studies of stellar content, gas distribution, and abundance gradients. It is also an ideal target to test chemical evolution models because it shows no signs of recent mergers and no presence of a prominent bulge (Regan & Vogel 1994; Bullock & Johnston 2005). Star counts in the outer disk

indicate that the stellar halo in this galaxy contributes for less than few percents to its total luminosity (Barker et al. 2007; McConnachie et al. 2006).

Quantitative comparisons between several observable quantities and model predictions are now possible in M33 thanks to: *i*) the recent identification of individual stars (Bolck et al. 2006; Barker et al. 2007) suggesting the existence of different episodes of star formation; *ii*) chemical abundance determinations in stellar populations of different ages (Magrini et al. 2004, 2007b; Urbaneja et al. 2005; Crockett et al. 2006; Barker et al. 2007); *iii*) surveys of molecular hydrogen through the CO J=1-0 line

*Send offprint requests to:* L. Magrini

(Engargiola et al. 2003; Heyer et al. 2004); *iv*) limits on stellar masses from dynamical mass modeling (Corbelli 2003).

## 2. The chemical evolution model

In this work we adopted a generalization of the multi-phase model (Ferrini et al. 1992), built for the solar neighborhood, and subsequently extended to the entire MW (Ferrini et al. 1994), and to other disk galaxies (Mollá et al. 1996, 1997, 2005). The main characteristics of this model are described in detail in Magrini et al. (2007a) and briefly summarized below. The galaxy is divided into  $N$  coaxial cylindrical annuli with inner and outer galactocentric radii  $R_i$  ( $i = 1, N$ ) and  $R_{i+1}$ , respectively, mean radius  $R_{i+1/2} \equiv (R_i + R_{i+1})/2$  and height  $h(R_{i+1/2})$ . Each annulus is divided into two *zones*, the *halo* and the *disk*, composed by diffuse gas  $g$ , clouds  $c$ , stars  $s$  and stellar remnants  $r$ .

The *halo* component represents the primordial baryonic halo and/or the material accreted from interactions with small LG galaxies or from the intergalactic medium during the lifetime of the galaxy. Each annulus is evolving independently (i.e. without radial mass flows) from  $t = 0$  to  $t_{\text{gal}} = 13.6$  Gyr.

The rate coefficients of the model describing the cloud formation and the star formation from different processes are all assumed to be independent of time but functions of the galactocentric radius  $R$  as discussed in detail for the MW case (Ferrini et al. 1994; Mollá et al. 1996, 2005).

### 2.1. The collapse and accretion models

Two class of models can be considered for M33, each corresponding to different gas infall rates through its cosmic evolution. The infall rate  $f$  has an exponential radial dependence with scalelength  $\lambda_D$

$$f(R) = f_0 \exp(-R/\lambda_D) \quad (1)$$

where  $f_0$  is the infall rate at  $R = 0$  (Ferrini et al. 1994; Portinari et al. 1999).

In the first class of models the disk is formed very rapidly at the beginning of a

galaxy's life (*collapse* model). In this kind of models, the infall coefficient  $f_0$  is usually set of the order of the inverse of the collapse time  $\tau_c$  for the galaxy, where  $\tau_c$  depends on the total mass of the galaxy  $M_{\text{Gal}}$  as  $\tau_c \propto M_{\text{Gal}}^{-1/2}$  (Gallagher et al. 1984). On the other hand, if the disk formation is a slow continuous accretion process from the environment (*accretion* model), lower values of  $f_0$  are needed. This second class of models imply a high infall rate at present time, and in general an infall rate almost constant through galaxy evolution. This is obtained for example setting  $f_0 \approx 0.003$ , corresponding to an infall rate of  $1.2 M_{\odot} \text{ yr}^{-1}$  in the disk of M33 at present time or about  $\dot{M}_{\text{inf}} \approx 3.8 M_{\odot} \text{ pc}^{-2} \text{ Gyr}^{-1}$ , averaged over the entire disk.

High infall rates, similar to those obtained with the *accretion* model, are favoured by some recent works describing the evolution of disk galaxies (Naab et al. 2006). Infall rate in the MW for example are predicted to be of order  $2\text{--}4 M_{\odot} \text{ yr}^{-1}$ , with little variations over the last 10 Gyr. These values are in good agreement with those inferred from observations of high velocity clouds and explain specific abundance patterns such as the high deuterium abundance at the solar neighborhood and at the Galactic Center (Chiappini et al. 2002). In addition, hydrodynamical simulations of galaxy formation and evolution show that accretion of 'cold' gas from intergalactic filaments becomes the dominant accretion process for low mass galaxies and in low density regions. Galaxies of mass similar to M33 should accrete gas at a rate which decreases slowly with time and is currently  $\approx 1 M_{\odot} \text{ yr}^{-1}$  (Keres et al. 2005). Deep 21-cm observations of the M33 region have moreover given some evidence of intergalactic gas material infalling on the M33 disk (Westmeier et al. 2005).

### 2.2. The evolution of the SFR

The radial profile and the magnitude of the SFR at the present epoch are important constraints to chemical evolution models. These observables allow to discriminate between different evolutionary scenarios that result in the

same radial distributions of stars, gas and chemical abundances.

In fact, both models, *collapse* and *accretion*, well reproduce the present time atomic and molecular gas distributions, and the stellar density profile of M33. Differences between the predictions of two models are more evident at earlier times, because the bulk of the stellar mass settles in the disk earlier in the *collapse* model than in the *accretion* model, due to the rapid gas infall and to the high star formation rate. The predicted SFR at present time is instead very different in the two models and the *accretion* model reaches a closer agreement with the present SFR inferred from observations (Heyer et al. 2004; Magrini et al. 2007a). In the *collapse* model the accretion rate and SFR vary more rapidly with time: as a consequence stars form earlier and the present-day SFR is at least a factor  $\sim 3$  lower than what can be inferred by infrared and optical observations. Clearly, the higher infall rate on the disk at present times for the *accretion* model results in a more vigorous SFR than in the *collapse* model. But at earlier times the SFR was higher for the *collapse* model, since the larger gas reservoir accreted earlier by the disk was rapidly converted into stars.

### 3. The time evolution of metallicity gradients

Both models we consider predict abundance gradients which flatten with time. The main difference between the two models is the value of the slope of the gradients, that are much steeper at all times in the *collapse* model than in the *accretion* model. This is due to the different nature of the infall: the *collapse* model predicts a much shorter time scale for the formation of the disk, due to a rapid collapse of the halo, while the *accretion* model predicts a continuous infall of material from the intergalactic medium.

In the case of M33, the best fit to the whole set of observations is obtained with our *accretion* model, i.e. with a model which has a self-consistent SFR and a continuous gas infall. This model does not exclude an early collapse phase of a galactic halo, but considers its

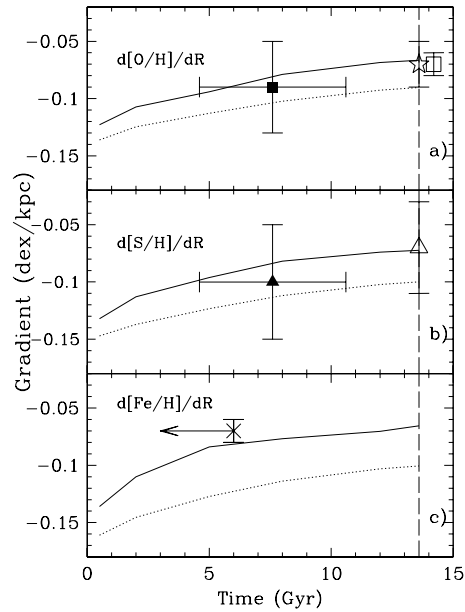


**Fig. 1.** The time evolution of the [O/H] (a), [S/H] (b), and [Fe/H] (c) gradients according to our *accretion* (continuous line) and *collapse* (dotted line) models, compared with gradient slopes of sulfur (*filled triangle*) and oxygen (*filled square*) of PNe, of sulfur (*empty triangle*) and oxygen (*empty square*) of HII regions and of iron of RGB stars (*cross*). The vertical dashed line marks the present age of the galaxy, 13.6 Gyr.

effects less important at the present time than the accumulation of matter from the intergalactic medium. Moreover, a continuous supply of gas is necessary to reproduce the high SFR observed at present time.

In Fig. 1 we compare the time evolution of the gradient of O/H (panel a), S/H (panel b), and Fe/H (panel c), predicted by both models, *accretion* and *collapse*, with the gradient measured in stellar population of different ages: young stars, HII regions, PNe, RGB stars. To derive the gradient, both the model predictions and the observational data have been linearly fitted in the  $\log[M/H]$ - $\log R$  plane, in the range of galactic radii 1–10 kpc. The amplitude of

the metallicity gradient predicted by the *accretion* model over the entire lifetime of the disk of M33 is quite modest because of the slow process of formation of the disk, which is still taking place at the present time. On the other hand, the *collapse* model predicts steeper gradients at all times, especially in the past, because of the rapid initial collapse phase that forms the inner disk in a few Gyr. Predictions of the *collapse* model are in conflict with the observations, especially with the Fe/H gradient of RGB stars (Barker et al. 2007), as shown in Fig. 1c.

The comparison of metal abundances in PNe with those in HII regions provides the first evidence for a flattening of the abundance gradients with time in an external galaxy. A similar result has been found in the MW (Maciel et al. 2006). The flattening in M33, particularly evident for O and S abundances, is due to the combination of the weak radial dependence of the infall rate and to the star formation efficiency which decreases more rapidly with time in the central regions. Another feature of particular interest in the case of M33 is the overall increase of metallicity with time at all radii. The steady infall rate, that increases the gas content of the disk with time, fuels star formation at all radii.

## References

- Barker, M. K., Sarajedini, A., Geisler, D., Harding, P., Schommer, R. 2007, *AJ*, 133, 1138
- Block, D. L., Puerari, I., Stockton, A. et al. 2006, *IAUS*, 235, 8
- Bullock, J. S., Johnston, K. V. 2005, *ApJ*, 635, 931
- Chiappini, C., Renda, A., Matteucci, F. 2002, *A&A*, 395, 789
- Corbelli, E. 2003, *MNRAS*, 342, 199
- Crockett, N. R., Garnett, D. R., Massey, P., Jacoby, G. 2006, *ApJ*, 637, 741
- Engargiola, G., Plambeck, R. L., Rosolowsky, E., Blitz, L. 2003, *ApJS*, 149, 343
- Ferrini, F., Matteucci, F., Pardi, C., Penco, U. 1992, *ApJ*, 387, 138
- Ferrini, F., Mollá, M., Pardi, M. C., Diaz, A. I., 1994, *ApJ*, 427, 745
- Freedman, W. L., Wilson, C. D.; Madore, B. F. 1991, *ApJ*, 372, 455
- Gallagher, J. S., III, Hunter, D. A., Tutukov, A. V. 1984, *ApJ*, 284, 544
- Heyer, M. H., Corbelli, E., Schneider, S. E., Young, J. S. 2004, *ApJ*, 602, 72
- Keres, D., Katz, N., Weinberg, D. H., Davè, R. 2005, *MNRAS*, 363, 2
- Maciel, W. J., Lago, L. G., Costa, R. D. D. 2006, *A&A*, 453, 587
- Magrini, L., Perinotto, M., Mampaso, A., Corradi, R. L. M. 2004, *A&A*, 426, 779
- Magrini, L., Corbelli, E., Galli, D., 2007a, *A&A*, arXiv:0704.3187
- Magrini, L., Vílchez, J. M., Mampaso, A., Corradi, R. L. M., Leisy, P. 2007b, *A&A*, arXiv:0705.3116
- McConnachie, A. W., Chapman, S. C., Ibata, R. A. et al. 2006, *ApJ*, 647, 25
- Mollá, M., Ferrini, F., Diaz, A. I. 1996, *ApJ*, 466, 668
- Mollá, M., Ferrini, F., Diaz, A. I. 1997, *ApJ*, 475, 519
- Mollá, M., Diaz, A. I. 2005, *MNRAS*, 358, 521
- Naab, T., Ostriker, J.P. 2006, *MNRAS*, 366, 899
- Portinari, L., Chiosi, C. 1999 *A&A*, 350, 827
- Regan, M. W., Vogel, S. N. 1994, *ApJ*, 434, 536
- Urbaneja, M. A., Herrero, A., Kudritzki, R.-P., Najarro, F., Smartt, S. J., Puls, J., Lennon, D. J., Corral, L. J. 2005, *ApJ*, 635, 311
- Westmeier, T., Braun, R., Thilker, D. 2005, *A&A*, 436, 101